ELSEVIER

Geomorphology 27 (1999) 131–150

GEOMORPHOLOGY

Estimates of the rate of regolith production using ^{10}Be and ^{26}Al from an alpine hillslope

Eric E. Small *, Robert S. Anderson, Gregory S. Hancock [1]

Department of Earth Sciences and Institute for Tectonics, University of California, Santa Cruz, CA 95064, USA

Received 6 May 1997; revised 17 February 1998; accepted 11 May 1998

Abstract

The production of regolith is a fundamental geomorphic process because most surface processes transport only unconsolidated material. We use concentrations of the cosmogenic radionuclides (CRNs) ^{10}Be and ^{26}Al in regolith and bedrock to deduce the rate of production of regolith on an alpine hillslope in the Wind River Range, WY. These calculations are based on a theoretical model which we develop here. This model shows that it is important to consider dissolution of regolith in regolith production and in basin-averaged erosion rate studies. Rates of production of regolith are uniform along the hillslope and the mean rates for the entire hillslope deduced from ^{10}Be and ^{26}Al are 14.3 ± 4.0 and 13.0 ± 4.0 m Ma^{-1}, respectively. Rates of production of regolith deduced from ^{10}Be concentrations in regolith-mantled bedrock support the rates deduced from regolith concentrations. In the alpine environment examined here, the rate of production of regolith beneath $\sim$ 90 cm of regolith is nearly twice as fast as the average rate of production of regolith on bare rock surfaces, which Small et al. [Small, E.E., Anderson, R.S., Repka, J.L., Finkel, R., 1997. Erosion rates of alpine bedrock summit surfaces deduced from in situ ^{10}Be and ^{26}Al. Earth and Planetary Science Letters 150, 413–425] previously documented. Rock-mantled with regolith probably weathers more rapidly than bare rock because the water required for frost weathering is limited on bare rock surfaces. Because the hillslope examined here is convex with constant curvature and regolith production and thickness are uniform down the slope, the regolith volume flux must be proportional to the local slope of the hillside. Therefore, our results are consistent with Gilbert's [Gilbert, G.K., 1909. The convexity of hilltops. Journal of Geology 17, 344–350] steady state hillslope hypothesis. If tor height and the difference between rates of weathering on bare and regolith-mantled rock provide a fair estimate of the age of summit flats, steady-state hillslope conditions have been attained in less than several million years.

Keywords: regolith production; Alpine hillslope; regolith-mantled rock; bare rock

1. Introduction

The transformation of bedrock to regolith, or the production of regolith, is a fundamental geomorphic process because most surface processes are only capable of transporting unconsolidated material.

* Corresponding author. Present address: Department of Earth and Environmental Sciences, New Mexico Tech., Sco Socorro, NM 87801, USA; E-mail: esmall@nmt.edu

[1] Now at Department of Geology, College of William and Mary, Williamsburg, VA 23187, USA.

0169-555X/99/$ - see front matter
PII: S0169-555X(98)00094-4

Rates of regolith production are, therefore, valuable for understanding several components of geomorphic systems. First, where the production of regolith is limited or is balanced by erosion (the weathering limited case), the rate of erosion is synonymous with the rate of regolith production. Second, it has been hypothesized that the rate of production of regolith is dependent upon the local thickness of regolith (e.g., Gilbert, 1877). The dependence of the rate of regolith production on the depth of regolith in a variety of climatic settings should reveal the controls on the processes of regolith production. This is critical for understanding the style and pace of long term landscape evolution. Third, transport velocities on hillslopes, and the relationship between the transport velocity on a hillslope and slope steepness, can be calculated from rates of regolith production on hillslopes whose thickness of regolith is steady. Fourth, rates of production of regolith are required to test the hypothesis of Gilbert (1909) that some hillslopes exist in a state of dynamic equilibrium.

Gilbert (1909) proposed that commonly observed convex hilltops are in dynamic steady state, meaning that neither the topographic form nor the thickness of regolith are changing through time even though erosion removes material from the hillslope. He reasoned that a regolith balance exists at each point along the hillslope: production of regolith by weathering at the bedrock interface must equal the divergence of downslope transport. Further, if the production of regolith or rate of weathering is uniform, then there must be a linear increase of regolith transport rate with distance from the crest. Because we commonly observe convex slopes, in which the slope increases linearly with distance from the crest, implies that the slope is adjusted to enable this increase in flux with distance, and that the rate of regolith transport is proportional to surface slope. This conceptual model of hillslope evolution has rarely been tested on long time scales.

Previous direct measurements of the rate of production of regolith have been limited, as have measurements of long term rates of transport. Monaghan et al. (1992) and McKean et al. (1993) used ^{10}Be produced in the atmosphere ('garden variety' ^{10}Be) to constrain creep velocities on a convex hillslope in the California coast range. Assuming that the hillslope form and the thickness of regolith are steady, they then calculated the necessary rate of regolith production that would be required to accommodate the divergence of hillslope flux. Their data were consistent with Gilbert's dynamic equilibrium hillslope hypothesis. Recently, Heimsath et al. (1997) used ^{10}Be and ^{26}Al to show that the production of soil declines exponentially with increasing soil depth on several hillslopes in northern California.

In situ produced cosmogenic radionuclides (CRNs) have recently been used for various Quaternary history and geomorphic applications (Bierman, 1994), including surface-exposure age dating and weathering and erosion studies. CRN analyses are valuable for studying long term rates of geomorphic processes because the concentration of a CRN in a sample represents 10^3–10^6 years of exposure history. Here we use CRN concentrations in regolith and bedrock to deduce rates of production of regolith from alpine environments in the Wind River Range, WY (Fig. 1). Because any interpretation of CRN concentrations relies upon a model of the CRN production history to which the sample has been subjected (Bierman, 1994; Hallet and Putkonen, 1994; Small et al., 1997), we first develop the theoretical model that we use to deduce rates of regolith production from CRN concentrations. This model explicitly accounts for dissolution of regolith, which we show is also important to consider in studies of basin-averaged erosion rates. Second, we discuss the sampling site and procedures. Finally, we use our

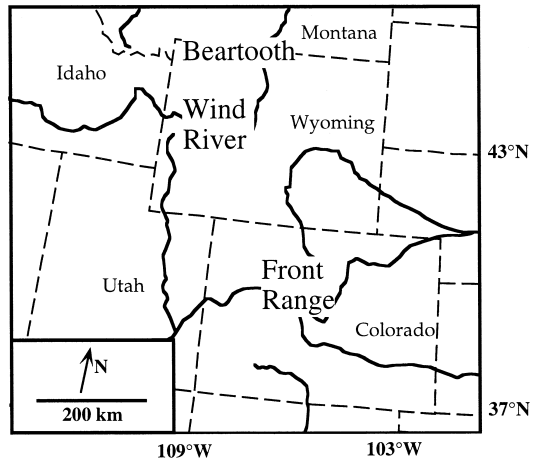

Fig. 1. Location of the mountain ranges in the Western US where CRN erosion rate samples were collected.

results to: (1) calculate rates of regolith production, rates of hillslope transport, and values of landscape diffusivity; (2) test the applicability of the hypothesis of Gilbert (1909) of dynamic equilibrium on hillslopes; and (3) compare rates of regolith production reported here with previously reported rates of bare rock erosion from the same environment.

2. Theoretical background

CRNs are formed when target nuclei are bombarded by high-energy cosmic ray particles (Lal and Peters, 1967). Silicon is a potential target nucleus for in situ production of ^{26}Al ($t_{1/2} = 0.7$ Ma) and oxygen is a potential target nucleus for in situ production of ^{10}Be ($t_{1/2} = 1.5$ Ma). Here we measure ^{26}Al and ^{10}Be in quartz, produced by interactions with these nuclei. The production of CRNs within materials decreases exponentially with depth:

$$P(z) = P_0 e^{-z/z^*} \quad (1)$$

where the scale length, $z^* = \Lambda/\rho$, is the ratio of the absorption mean-free path, Λ, of ~ 155–160 g cm^{-2} and the density of the solid, ρ (Brown et al., 1992; Nishiizumi, 1994).

To use regolith CRN concentrations to constrain rates of production of regolith, we combine mass and CRN balances for the regolith. We explicitly account for the abundance of quartz in bedrock and regolith because we measure the CRNs within quartz. We make two fundamental assumptions that affect the mass and CRN balances: (1) the thickness of regolith is steady over the interval sampled by CRNs; and (2) regolith is fully-mixed between the bedrock–regolith interface and the surface. The importance of these assumptions is outlined below. Our approach is similar to that of Monaghan et al. (1992) but it differs from theirs in that (1) we are using in situ CRNs, and, therefore, must account for the abundance of quartz, and (2) we include the effects of dissolution within the regolith.

2.1. Total and quartz mass balance

We first develop total and quartz mass balances for regolith. The total mass balance for regolith between the hillcrest ($x = 0$) and a point down the hillslope ($x = L$) is (Fig. 2):

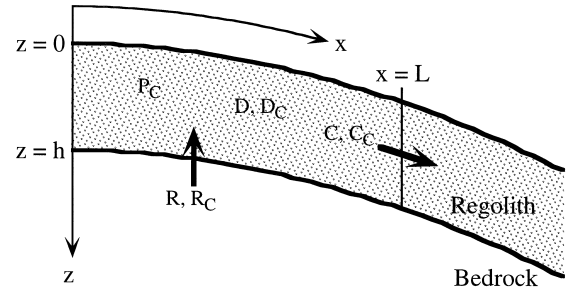

Fig. 2. This scheme was used to evaluate hillslope mass (total and quartz) and CRN balance. No subscript indicates component of mass balance. Subscript (C) indicates component of CRN balance. Regolith production (R) adds mass and CRNs to the hillslope element, whereas regolith dissolution (D) and regolith creep (C) remove mass and CRNs. In addition, in situ production (P) of CRNs within the regolith adds CRNs.

$$\int_0^L R(x)\,dx = \rho_R \int_0^h u(L,z)\,dz + \int_0^L \int_0^h D_R(x,z)\,dz\,dx. \quad (2)$$

This mass balance is based on the assumptions that the thickness of regolith, h, is steady and that no topographic divergence occurs out of the plane of the cross-section $(1 - D)$. R is the rate of production of regolith from bedrock (g cm^{-2} year^{-1}), ρ_R is the density of regolith (g cm^{-3}), u is the downslope creep rate of regolith (cm year^{-1}), and D_R is the rate of mass removal by chemical weathering processes in the regolith (g cm^{-3} year^{-1}), which we refer to as the rate of regolith dissolution. Regolith dissolution removes mass from the regolith in the form of solutes, which are the product of a variety of chemical weathering processes. For the remainder of this paper, we assume that D_R is uniform with distance along the hillslope. Eq. (2) can be written using the vertically-averaged downslope creep rate of regolith, $\hat{u}$, and the vertically-averaged rate of dissolution of regolith, $\hat{D}_R$. Both $\hat{u}$ and $\hat{D}_R$ represent average values between the bedrock–regolith interface and the surface. Eq. (2) then becomes:

$$\int_0^L R(x)\,dx = \rho_R\,\hat{u}(L)\,h + \hat{D}_R\,hL. \quad (3)$$

The regolith dissolution rate is related to the dissolution rates of the quartz, $\hat{D}_R^q$, and non-quartz, $\hat{D}_R^{nq}$, components of the regolith as follows:

$$\hat{D}_R = (1 - f_R)\,\hat{D}_R^{nq} + f_R\,\hat{D}_R^q \quad (4)$$

where f_R ($g_q\ g_R^{-1}$) is the mass fraction of quartz in regolith. By definition, the mean rate of regolith production between the hillcrest ($x = 0$) and some point downslope ($x = L$) is:

$$\langle R\rangle(L) = \frac{1}{L}\int_0^L R(x)\,\mathrm{d}x. \quad (5)$$

Combining Eqs. (3) and (5), and assuming that h is uniform between the hillcrest and $x = L$:

$$\langle R\rangle(L) = \frac{1}{L}\rho_R\,\hat{u}(L)\,h + \hat{D}_R h. \quad (6)$$

A similar balance can be written for quartz only, again assuming that the rate of chemical dissolution is spatially uniform:

$$f_B\int_0^L R(x)\,\mathrm{d}x = f_R\rho_R\,\hat{u}(L)\,h + f_R\hat{D}^{qR}hL \quad (7)$$

where f_B ($g_q\ g_B^{-1}$) denotes the mass fraction of quartz in bedrock. Again, this balance is based on the assumption that the thickness of regolith is steady. The assumption of fully-mixed regolith permits us to use vertically averaged values for creep and dissolution. Without this assumption, we would need to know the vertical pattern of f_R and vertical changes in the creep and dissolution rates to appropriately calculate removal of quartz from the hillslope element. Our results indicate this assumption is generally valid (discussed below). Again, the average rate of regolith production is:

$$f_B\langle R\rangle(L) = f_R\frac{1}{L}\rho_R\,\hat{u}(L)\,h + f_R\hat{D}^{qR}h. \quad (8)$$

Eqs. (6) and (8) can be combined to show how the ratio of the fraction of quartz in regolith and bedrock depends on the rate of regolith production, rates of dissolution of quartz and non-quartz regolith, and on the thickness of soil.

$$\frac{f_R}{f_B} = \frac{\langle R\rangle(L)}{\langle R\rangle(L) + h\left[\hat{D}_R^q - \hat{D}_R\right]} \quad (9a)$$

$$\frac{f_R}{f_B} = \frac{\langle R\rangle(L)}{\langle R\rangle(L) - h\hat{D}_R} \quad (9b)$$

Eq. (9b) is the result if we assume that the rate of chemical dissolution of the quartz fraction of the regolith is zero. No enrichment of quartz occurs in the regolith ($f_R/f_B = 1$) if the rate of dissolution of quartz and the total rate of regolith dissolution are either both zero or are equal.

2.2. Cosmogenic balance

We now write the balance of in situ produced CNRs, such as ^{10}Be or ^{26}Al, for the regolith, assuming that the concentration in the regolith is steady and that decay of CRNs is not important. Our results (described below) show that the no-decay assumption is valid for the hillslope we examine here. A CRN balance in the regolith includes (Fig. 2): (1) addition by in situ CRN production within the regolith, P_R; (2) addition associated with the transformation of bedrock to regolith, P_{RP}; (3) dissolution of CRN-bearing quartz, S_D; and (4) removal by regolith creep, S_C.

$$P_R + P_{RP} = S_D + S_C \quad (10)$$

All fluxes are weighted by the mass fraction of quartz, because it is ^{10}Be and ^{26}Al in quartz that we measure here. We now derive each of the terms in Eq. (10).

2.2.1. CRN production within the regolith

The in situ production rate of CRNs in regolith, P_R (atoms cm^{-1} year^{-1}), within a hillslope element between the hillcrest and $x = L$ is:

$$P_R(L) = f_R\rho_R h\int_0^L \hat{P}(x)\,\mathrm{d}x \quad (11)$$

where $\hat{P}$ is the mean production rate throughout the regolith (atoms g_q^{-1} year^{-1}). The production rate decreases with depth in the regolith, with an exponential length scale $z_R^* = \Lambda/\rho_R$. Assuming that the surface production rate, P_0, is uniform with distance along the hillslope, the mean production rate within the regolith is:

$$\hat{P}(x) = \frac{1}{h}\int_0^h P_0 e^{\left(\frac{-z}{z_R^*}\right)}\mathrm{d}z = \frac{P_0 z_R^*}{h}\left[1 - e^{\left(\frac{-h}{z_R^*}\right)}\right]. \quad (12)$$

This assumption is valid considering the low slope-angles and small elevation changes considered here. The addition of CRNs by production within the regolith upslope from $x = L$ is then:

$$P_R(L) = f_R P_0 \Lambda L \left[1 - e^{\left(\frac{-h}{z_R^*}\right)}\right]. \quad (13)$$

2.2.2. Addition from regolith production

The addition of CRNs to the regolith arising from the transformation of bedrock to regolith, P_{RP} (atoms cm^{-1} $year^{-1}$), within a hillslope element results from regolith production from bedrock that has a particular concentration of CRNs, N_B (atoms g_q^{-1}):

$$P_{RP}(L) = f_B \int_0^L N_B(x)\, R(x)\, dx. \quad (14)$$

The concentration of CRNs in rock at the bedrock–regolith interface, N_B, depends on the rate at which the parcel of bedrock is 'unshielded', the surface CRN production rate, and the 'density' of the regolith:

$$N_B(x) = \frac{P_0 \Lambda e^{\left(\frac{-h}{z_R^*}\right)}}{R(x)}. \quad (15)$$

When the thickness of the soil remains constant, parcels of bedrock are 'unshielded' at a rate which is the sum of the rate of regolith production and the rate of bedrock dissolution integrated between the position of the rock at some time and the bedrock–regolith interface. We assume that the component of unshielding toward the surface from bedrock dissolution is zero. The result of this assumption is that the bedrock CRN concentration, N_B, and, therefore, the addition of CRNs from regolith production, P_{RP}, are overestimated, because bedrock dissolution increases the rate at which a rock parcel is unshielded and, therefore, decreases its exposure time and CRN concentration. Combining Eqs. (14) and (15), the addition of CRNs from regolith production is:

$$P_{RP}(L) = f_B P_0 \Lambda L e^{\left(\frac{-h}{z_R^*}\right)}. \quad (16)$$

2.2.3. Removal by dissolution

Dissolution of quartz in regolith with in situ CRNs, S_D (atoms cm^{-1} $year^{-1}$), removes CRNs from the hillslope element:

$$S_D(L) = f_R \hat{D}_R^q h \int_0^L \hat{N}_R(x)\, dx \quad (17)$$

where $\hat{N}_R$ is the vertically averaged CRN concentration within the regolith. To evaluate $S_D(L)$, which is required for the CRN balance of the hillslope element, we need to know how $\hat{N}_R$ varies along a hillslope (or the mean concentration over $x = [0, L]$). Because our goal is to calculate the rate of production of regolith between the hillcrest and L based on the CRN concentration at L, this information is not available. We consider two different assumptions to avoid this problem. The first is that dissolution of quartz in regolith is negligible, $\hat{D}_R^q \ll \hat{D}_R^{nq}$. This is probably a fair assumption in many environments because quartz is relatively resistant to chemical weathering, compared to other minerals (e.g., Lasaga et al., 1994). The second assumption is that $\hat{N}_R(x)$ is uniform along the hillslope, which makes it possible to evaluate $S_D(L)$ and include dissolution of CRN-bearing quartz in the CRN balance. This assumption closely describes the hillslope examined here (shown below), and may also be suitable in other situations. This second assumption is only useful for evaluating errors associated with dissolution, as the resulting equation cannot be used to calculate the rate of regolith production between the hillcrest and L based on the CRN concentration at L.

2.2.4. Removal by creep

The removal of CRNs from a hillslope element by regolith creep is (atoms cm^{-1} $year^{-1}$):

$$S_C(L) = f_R \rho_R h \hat{u}(L)\, \hat{N}_R(L). \quad (18)$$

The assumption of fully-mixed regolith permits the use of the vertically-averaged creep velocity, $\hat{u}$. Assuming that dissolution of quartz is negligible, the above equations can be combined to produce an equation for the CRN balance in a hillslope element:

$$f_R P_0 \Lambda L \left[1 - e^{\left(\frac{-h}{z_R^*}\right)}\right] + f_B P_0 \Lambda L e^{\left(\frac{-h}{z_R^*}\right)} = f_R \rho_R h \hat{u}(x)\, \hat{N}_R(x). \quad (19)$$

2.3. Regolith CRN concentration

This CRN balance can be combined with Eqs. (8), (9a) and (9b) to yield the relationship between the (measurable) CRN concentration of fully-mixed regolith at some point on a hillslope ($x = L$) and the desired rates of regolith production and dissolution upslope from that point. When regolith dissolution is non-zero, but dissolution of the quartz-component of the regolith is zero, $f_R \neq f_B$; $\hat{D}_R \neq \hat{D}_R^q = 0$:

$$\hat{N}_R(L) = \frac{P_0 \Lambda}{\langle R \rangle(L)} \left\{ \frac{f_R}{f_B} \left(1 - e^{\left(\frac{-h}{\frac{*}{z_R}}\right)} \right) + e^{\left(\frac{-h}{\frac{*}{z_R}}\right)} \right\} \tag{20a}$$

or:

$$\hat{N}_R(L) = \frac{P_0 \Lambda}{\langle R \rangle(L)} \left\{ \left[\frac{\langle R \rangle(L)}{\langle R \rangle(L) - h\hat{D}_R} \right] \times \left[1 - e^{\left(\frac{-h}{\frac{*}{z_R}}\right)} \right] + e^{\left(\frac{-h}{\frac{*}{z_R}}\right)} \right\}. \tag{20b}$$

If dissolution of quartz in the regolith is substantial ($\hat{D}_R \neq \hat{D}_R^q \neq 0$), then Eqs. (20a) and (20b) are not valid because dissolution of CRN-bearing quartz was not included in the CRN balance. Using the assumption that $\hat{N}_R(x)$ is uniform along the hillslope, we obtain a result similar to that in Eq. (20b), except that f_R/f_B has been replaced by the quantity in Eq. (9a).

$$\hat{N}_R(L) = \frac{P_0 \Lambda}{\langle R \rangle(L)} \left\{ \left[\frac{\langle R \rangle(L)}{\langle R \rangle(L) - h\left(\hat{D}_R - \hat{D}_R^q\right)} \right] \times \left[1 - e^{\left(\frac{-h}{\frac{*}{z_R}}\right)} \right] + e^{\left(\frac{-h}{\frac{*}{z_R}}\right)} \right\}. \tag{21}$$

The final and most simple case is when no chemical dissolution occurs in the regolith, $\hat{D}_R = \hat{D}_R^q = 0$, or when regolith and quartz-component of the regolith dissolution are equal and non-zero, $\hat{D}_R = \hat{D}_R^q \neq 0$. In both cases, no enrichment of quartz occurs in the regolith, $f_R/f_B = 1$, yielding:

$$\hat{N}_R(L) = \frac{P_0 \Lambda}{\langle R \rangle(L)}. \tag{22}$$

This solution is identical to that used for deducing basin-averaged rates of erosion from CRN concentrations (Brown et al., 1995; Bierman and Steig, 1996; Granger et al., 1996) except that we have replaced the basin-averaged rate of erosion with the hillslope averaged rate of regolith production in the denominator. As discussed above, the rate of production of regolith equals the rate of erosion when the thickness of regolith is steady. The one-dimensional approach that we describe here can be generalized for two dimensions, to show how the regolith CRN concentration depends on the rate of regolith production from a basin. We invert Eq. (22) to yield the mean rate of regolith production. This value represents the mean rate of regolith production from all points upslope from a sampling site. A local rate of regolith production, which represents the mean rate between adjacent sampling sites, can be calculated from the mean rates at the two sites.

2.4. Errors associated with regolith dissolution

If quartz is enriched in the regolith ($f_R > f_B$) by dissolution of other minerals, rates of regolith production calculated using Eq. (22) will be too low. The difference between actual and calculated rates of regolith production increases with greater quartz enrichment (Fig. 3a). For example, if the actual rate of production of regolith is 15 m Ma^{-1}, the calculated rate will be 10.8 m Ma^{-1} if $f_R/f_B = 1.5$ compared to 8.5 m Ma^{-1} if $f_R/f_B = 2.0$. The magnitude of the error also increases for greater values of regolith thickness (Fig. 3b). These errors are substantial compared to other errors associated with the CRN method (e.g., production rate, analytical, etc.). For example, regolith quartz enrichment of 1.5 results in an error of 20–30% depending on the thickness of regolith. This magnitude of quartz enrichment is reasonable if f_B is relatively low. For example, if f_B is 0.3 in granitic rock, enrichment of 1.5 would produce a quartz fraction in regolith of 0.45. Errors associated

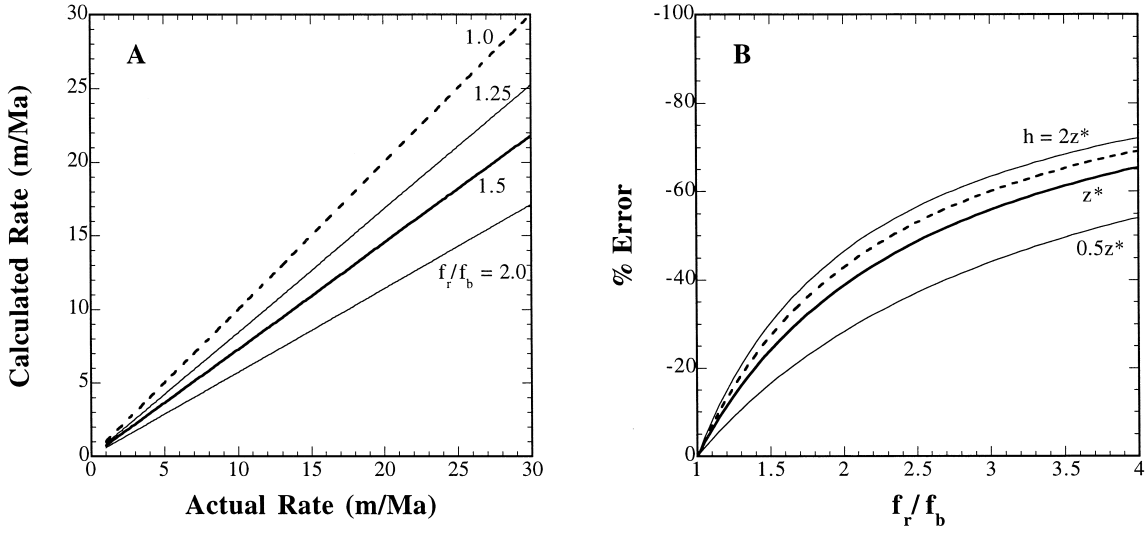

Fig. 3. (A) The rate of regolith production calculated using Eq. (22) compared to the actual rate of regolith production (Eqs. (20a) and (20b)) for various values of f_R/f_B. Each line is calculated using regolith thickness of 1.0 m and z^* of 0.72 m. (B) The percent error that results from assuming that regolith dissolution is zero as a function of quartz enrichment (f_R/f_B). The different lines show various thicknesses of regolith. Solid lines (labeled) are for h/z^* of 2.0, 1.0, and 0.5. The dashed line shows the relationship for regolith thickness of 1.0 m and z^* of 0.72 m, which are the appropriate values for the hillslope examined here. Percent error is calculated as [100 × (calculated − actual)/actual].

with selective dissolution in regolith will be minor in rocks with high values of f_B (e.g., quartzite), because substantial enrichment of quartz in the regolith is not possible. In most geomorphic environments and for most rock types, we expect that $f_R/f_B > 1.0$, and that rates of regolith production calculated with Eq. (22) will therefore be lower than the true values. In the unlikely case that $f_R/f_B < 1.0$, the rate of production of regolith calculated using Eq. (22) would be higher than the actual rate.

2.5. Regolith dissolution and basin-averaged rates of erosion

Recently, it has been shown that CRN concentrations in fluvial sediments can be used to deduce basin-averaged rates of erosion (Brown et al., 1995; Bierman and Steig, 1996; Granger et al., 1996). In these analyses, it is explicitly assumed that fluvial transport time is ~ 0.0, so that the CRN concentration of quartz in fluvial sediments represents the mean CRN concentration of quartz in regolith throughout the basin. Our analysis shows that changes in the fraction of quartz between bedrock and regolith, resulting from selective dissolution of regolith, alters the CRN concentration in regolith quartz, and, therefore, the CRN concentration of quartz in fluvial sediments. Basin-averaged rates of erosion, deduced from CRN concentrations in fluvial sediments, will be affected by the same selective dissolution-related errors as rates of regolith production.

Here we show where one of the three previously mentioned methods to deduce basin-averaged rates of erosion implicitly assumes that no quartz enrichment occurs, and how selective dissolution of regolith affects basin-averaged rates of erosion. For a well-mixed regolith profile, the CRN concentration throughout the regolith is equal to the surface CRN concentration of a bedrock surface eroding at the same rate (Brown et al., 1995; Granger et al., 1996). Therefore, the equation for rapid (no-decay) bedrock erosion ($N = P_0 \Lambda/\varepsilon$) (where ε is g cm^{-2} year^{-1}) (Lal, 1991) can be used to deduce rates of erosion from mean regolith CRN concentrations (Granger et al., 1996). Granger et al. (1996) implicitly assume that the bulk regolith and quartz fraction rates of dissolution are equal (or both zero), as they state that the time quartz remains in the regolith equals the soil

thickness (assumed steady) divided by the erosion rate, $t_R = h/\varepsilon$. However, the quartz residence time in the regolith is only h/ε if the rates of dissolution of quartz and non-quartz components of the regolith are equal. Allowing for dissolution of non-quartz minerals within the regolith, the time quartz remains in the regolith is:

$$t_R^q = \frac{h}{R}\frac{f_R}{f_B} = \frac{h}{\varepsilon}\frac{f_R}{f_B} = \left[\frac{h}{R - h\hat{D}_R}\right]. \quad (23)$$

Substituting this equation for t_R into Eq. (2) of Granger et al. (1996) yields our Eq. (20b), which reflects the relationship between regolith CRN concentration, regolith production (or erosion), and dissolution of regolith. A similar substitution could be made using the relationship for f_R/f_B when dissolution of quartz in regolith is non-zero (Eq. (9a)), which would yield our Eq. (21). We conclude that errors associated with selective dissolution of regolith should be addressed in studies of basin-averaged erosion.

3. Study area and sampling sites

3.1. Study area

While we focus on the Wind River Range of Wyoming, our results are pertinent to the processes and forms of several other Laramide Ranges within western North America. We have previously reported rates of bare-bedrock erosion from the Wind River and Beartooth Ranges, WY, as well as the Front Range, CO (Small et al., 1997; Fig. 1). All of these ranges have several features in common. First, crystalline bedrock (granite or gneiss) is abundant at the highest elevations in each range. Second, valleys were intermittently glaciated during the Pleistocene (Porter et al., 1982). Third, many of the highest peaks and ridges in each range are capped by extensive low-relief surfaces (which we refer to as 'summit flats') that show no evidence of past glaciation (Fig. 4).

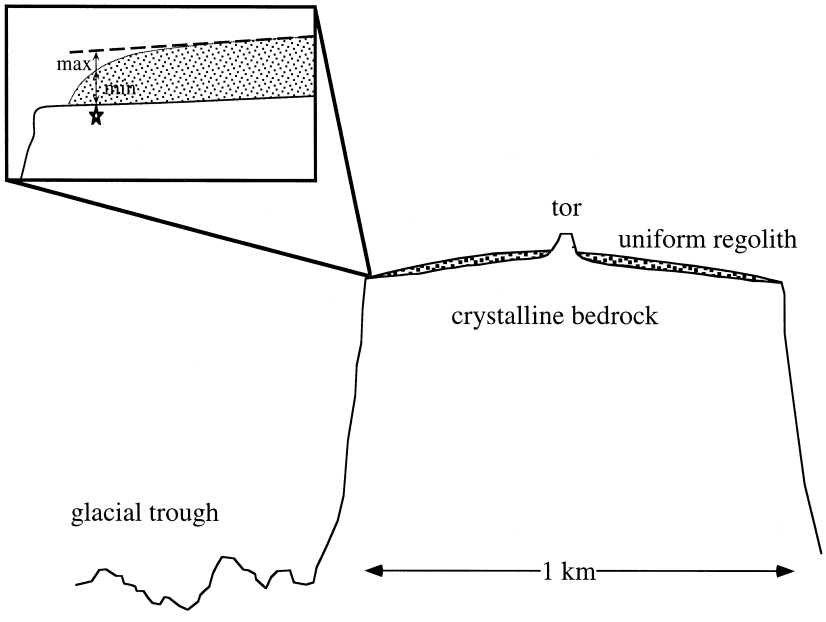

Fig. 4. Sketch of a typical summit flat. The stippled pattern represents regolith, unfilled areas are bedrock. Inset shows detail of summit flat edge, where bedrock samples were collected (denoted by star). The minimum (min) and maximum (max) possible thickness of regolith at the sample location are shown. The maximum possible thickness is estimated by linearly projecting the surface profile to the location of the sample (dashed line).

3.2. Summit flats

Summit flats share many features in common among these three ranges (Fig. 4). Summit flats rarely exceed several square kilometers in area. They are largely convex with uniform curvature, and display unchanneled low angle (typically 2–3°, maximum 10°) hillslopes up to 1 km long. Road-cuts and hand-dug pits reveal that the thickness of regolith is usually about 1 m. At the edges of summit flats, the thickness of regolith commonly feathers to zero, exposing a several-meter wide bare bedrock bench. Bedrock cliffs, several hundred meters high, isolate these surfaces from the glaciated troughs below. Hillslopes appear to be dominated by periglacial processes; sorted nets and stripes, felsenmeer, and nivation hollows are common.

We recognize no evidence of prior glaciation on any of the summit flats. Glacial striations and erratic boulders are absent. Boulders composed of a distinctive lithology can be traced to nearby, upslope bedrock sources. Summit flats are much smoother than the surfaces of the glaciated troughs below, where roche moutonée, other bedrock bumps, and overdeepenings ornament and complicate the broadly u-shaped valley floors. The bedrock surface underlying summit flats, which is exposed in canyon walls, is smooth at length scales greater than several meters. It is not simply a rough bedrock landscape mantled by a smoothing regolith. Also, no evidence exists of either past or modern fluvial channelization. The low slopes of summit flats inhibit erosion by discrete landslides. Cliff retreat at the edges of summit flats reduces the area, but does not lower the surface elevation. The absence of glacial, fluvial, or landsliding processes implies that erosion of summit flats is dominated by frost creep. Therefore, the erosion of summit flats must be limited by the rate of production of regolith, because creep only transports unconsolidated material.

Tors (bedrock knobs that protrude through the mantle of regolith) are abundant along the crests and edges of summit flats. The height of tors varies between several and $\sim$ 15 m. Vertical and horizontal joint sets, with $\sim$ 0.2–2 m spacing, disrupt all of the tors we examined. Numerous blocks, which have become detached from the bedrock along joint surfaces, blanket the flanks of tors. These blocks have toppled into various orientations and extend 10 s of m from the tors and create a felsenmeer apron. The bedrock surface of tors is frequently defined by joint planes, which sometimes can be traced within adjacent intact bedrock. The dimensions, orientations, and distribution of the detached blocks and the presence of joint planes at the bedrock surface all suggest that vertical and horizontal erosion of tors proceeds by the removal of distinct joint blocks. Minor numbers of small clasts and amounts of sand indicate that erosion by granular disintegration occurs, but is far less important than the removal of blocks. Most bedrock surfaces lack relief at the centimeter and finer scales, suggesting that dissolution is locally not an effective erosion process. We saw no evidence of the fine scale flutes and pits associated with ventifaction.

The morphology of summit flats raises several questions relevant to the evolution of such alpine settings, including: (1) is the erosion of summit flats slower than erosion in adjacent valleys, indicating that relief is increasing?; (2) are summit flat hillslopes steady state forms, as defined by Gilbert (1909)?; (3) are the tors growing in amplitude—i.e., is the regolith-mantled surface, and the bedrock–regolith interface if the thickness of soil is steady, downwearing at a rate that is greater than that of bare bedrock tors?

3.3. Sampling strategy

We address these questions by incorporating analyses of CRN concentrations in regolith and bedrock into the model described above. We collected regolith CRN samples parallel to the direction of maximum curvature over a convex hillslope in the Wind River Range (lat 43.37°N, long 109.75°W) (Fig. 5). The elevation of the hillslope is $\sim$ 3600 m. The slope increases nearly linearly with distance from the hillcrest (curvature $\approx 0.007\ m^{-1}$), except where the surface profile is interrupted by $\leq$ 0.5 m amplitude bumps and swales. The shape of the hillslope is uniform for $\sim$ 200 m perpendicular to the profile direction, so minimal topographic divergence occurs along the profile. In places where we excavated pits (Fig. 5), the granitic bedrock was covered by $\sim$ 1 m of regolith. The regolith is composed primarily of a sand/slit matrix with larger clasts contributing

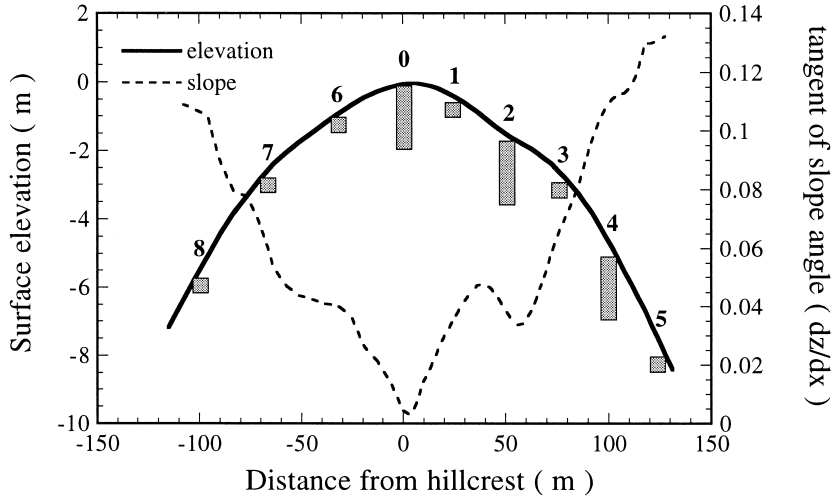

Fig. 5. Surface profile and local slope across hillslope in Wind River Range. Profile runs nearly north–south (positive x-values are north). Reference number (see Table 1) and location of surface samples (squares) and depth profiles (rectangles) along hillslope are shown. Depth to regolith–bedrock interface at the three depth profiles is 90 cm at $x = 0$ m, 103 cm at $x = 50$ m, and 92 cm at $x = 100$ m.

~ 30% by volume. We did not visually observe any continuous vertical or downslope changes in this grain-size distribution; however, we did notice some downslope variability in sorting at the several meters of length scale. This sorting was spatially associated with the bumps and swales that interrupt the smooth surface profile, and we believe is from periglacial processes. About 20% of the surface is covered with sedges and lichen. We collected samples from vertical profiles (surface to just above the bedrock–regolith interface) at the hillcrest, and at 50 and 100 m down the northern side of the hillslope. In addition, we collected surface regolith from intermediate positions on the northern side of the hillslope, and at 33 m intervals on the south side (Fig. 5).

We collected two samples of regolith-mantled bedrock exposed at cliff edges within 1 km of the sampled hillslope, and one exposed in a roadcut in the Beartooth Range. All three samples were located along convex hillslopes similar to the one described above. We were unable to measure directly the long term thickness of overlying material from the Wind River bedrock samples because we suspect that cliff retreat has altered the original surface profiles (Fig. 4). We were able to constrain maximum possible values for the thickness of regolith, however, by surveying the hillslopes perpendicular to the cliff and linearly projecting the surface profile to the cliff edge. In addition, the present thickness of regolith provides a minimum estimate of the thickness prior to cliff retreat.

In addition, we compare the results from samples of regolith and regolith-mantled bedrock to previously reported results from exposed rock samples collected from tors and large boulders throughout the Wind River, Beartooth, and Front Ranges (Small et al., 1997).

4. Methods

4.1. Estimation of production rates

Local surface production rates, P_0, were calculated using the latitude-elevation coefficients of Lal (1991), the sea level high-latitude ^{10}Be production rate (4.8 atom g^{-1} year^{-1}) of Clark et al. (1995), and the ^{26}Al–^{10}Be sea-level production rate ratio (6.1) of Nishiizumi et al. (1989). Because our previous bare rock erosion rate estimates (Small et al., 1997) are based on production rate of Clark et al. (1995), we choose this value instead of the estimate of Nishiizumi et al. (1996) (5.8 atom g^{-1} year^{-1}). All rates of regolith production can be adjusted for

the Nishiizumi production rate by multiplying by a factor of 1.2. The effects of topographic shielding are negligible. For all the samples we measured, the topographic shielding factor (Nishiizumi et al., 1989) ranged from 0.99 to 1.00. At the elevation and latitude of the hillslope examined here, the production rates are 64 and 386 atom g^{-1} $year^{-1}$ for ^{10}Be and ^{26}Al, respectively.

4.2. Lab methods

We sieved dry regolith samples and used -4.0 to 2.25 ϕ. We crushed and sieved bedrock samples to a size of 1.25 to 2.25 ϕ. We separated quartz grains from other minerals with heavy liquid and magnetic separation techniques. Organics, Fe- and Mg-oxides, and carbonates were eliminated by heating for 24 h in a solution of 30% HCl and 1% H_2O_2. We then leached samples (>6 times) for 24 h in a 1% HF + 1% HNO_3 solution to remove any remaining non-quartz grains (Kohl and Nishiizumi, 1992), and to assure elimination of any atmospherically produced 'garden variety' ^{10}Be.

We added 0.5 mg of stable Be and Al to each 10–20 g quartz sample and dissolved the sample in concentrated HF. Stable aluminum concentrations were determined by inductively-coupled plasma mass spectrometry (ICP/MS) on an aliquot of the sample. Al and Be were separated by ion chromatography, precipitated as metal hydroxides, and then oxidized over a flame. In the Al_2O_3 or BeO form, the ratio of the radionuclide to the stable isotope was determined by accelerator mass spectrometry (AMS) at the LLNL/CAMS facility (Elmore and Phillips, 1987; Davis et al., 1990).

5. Results

5.1. Concentration with depth

^{10}Be and ^{26}Al concentrations are relatively uniform with depth into the regolith at each of the sampled locations (Fig. 6, Table 1). This implies that regolith is well-mixed. For a given rate of regolith production (or erosion), the concentration of CRN throughout fully-mixed regolith is equal to the surface CRN concentration of unmixed regolith or bedrock, regardless of the thickness of regolith (Brown et al., 1995; Granger et al., 1996), ignoring selective dissolution in the regolith. Alternatively, the CRN concentration of unmixed regolith or bedrock decreases exponentially with depth (e folding-scale $= z^*$), from a surface value determined by Eq. (22) (Lal, 1991) (Fig. 6).

CRN concentrations at the hillslope crest ($x = 0$ m) are nearly constant with depth. Based on both a t- and F-test of a least squares regression to the data, sufficient evidence does not exist at the 95% confidence level to show that the concentration changes with depth. The concentration at the base of the regolith ($z = 85$ cm) is about four times greater than the expected value if the regolith was completely unmixed. This indicates that the regolith is mixed to bedrock (~ 1 m), most likely by cryoturbation. With increasing distance down the hillslope, the concentration profiles become progressively less uniform with depth. At the two downslope depth profiles ($x = 50$ m and $x = 100$ m), the concentrations of the two uppermost samples are similar, whereas the concentrations decrease at greater depths. In both profiles, there is sufficient evidence at the 95% confidence level to show that CRN concentrations are not uniform with depth. The concentration at the regolith base, however, is still about three times greater than the unmixed value at the same depth. Whereas the data indicate that the regolith is not completely mixed at the two downslope depth profiles, the fully-mixed regolith assumption appears to be generally valid, especially when compared to the expected unmixed profiles.

5.2. Estimation of mean concentration from surface concentration

The mean rate of production of regolith can be deduced from the mean CRN concentration of fully-mixed regolith, which we have measured in the three depth profiles. We use the observed relationship between surface and mean regolith concentrations in the three depth profiles to estimate mean regolith concentrations from hillslope locations where only surface regolith was analyzed. We use a linear regression technique that propagates errors in both the

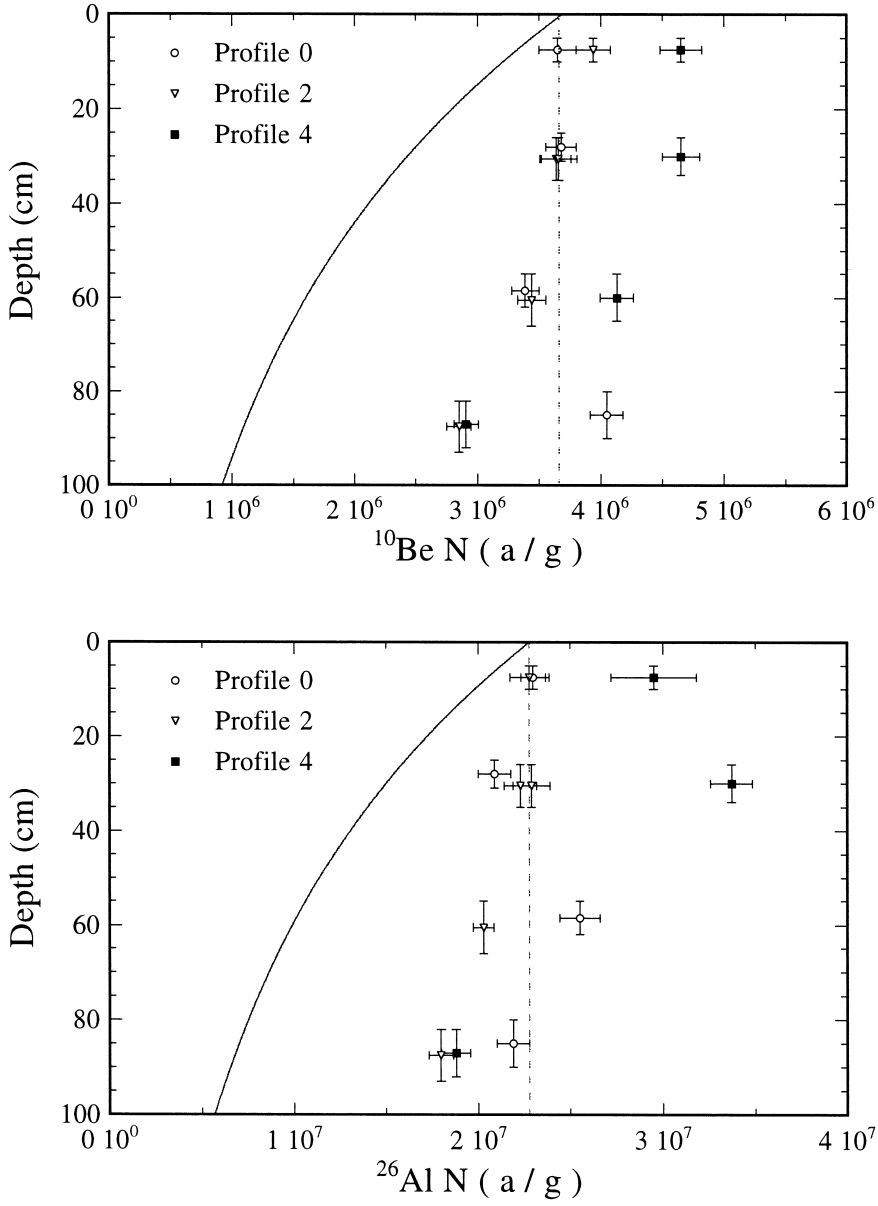

Fig. 6. Top: ^{10}Be concentration with depth into the regolith at depth profiles 0, 2, and 4 along the sampled hillslope. The vertical dashed line shows the mean concentration from the four samples in profile 0 ($^{10}\mathrm{Be} = 3.69 \times 10^6$ atom g^{-1}). The solid line represents the expected concentration with depth if the regolith was completely unmixed, with a surface value equal to the mean from profile 0. Constant regolith density is assumed ($z^* = 72$ cm). A repeat sample (not shown in Table 1) in depth profile 2 ($z = 30$ cm) is plotted. Error bars show 1σ analytical uncertainty. Bottom: same for ^{26}Al. Mean concentration of profile 0 (dashed line) is 2.28×10^7 atom g^{-1}.

mean and surface concentrations used to calculate the regression line and the surface concentrations from which we estimate mean values (York, 1966). The regression line is not forced through the origin.

Because surface and mean concentrations are nearly equal in the three depth profiles (fully-mixed assumption is a good approximation), the regression forces the estimated mean values to nearly match the

Table 1
^{10}Be and ^{26}Al data for hillslope regolith and buried rock samples

Sample (z is depth in centimeters)	Distance (m)	Concentration (10^6 atoms (g SiO_2)$^{-1}$)		Ratio ^{26}Al/^{10}Be	Mean regolith concentration (10^6 atoms (g SiO_2)$^{-1}$)		Minimum regolith production rate (m Ma^{-1})	
		^{10}Be	^{26}Al		^{10}Be	^{26}Al	^{10}Be	^{26}Al
Profile 0	0				3.69 ± 0.13	22.8 ± 0.88	13.9 ± 1.5	13.7 ± 1.5
$z = 7.5 \pm 2.5$		3.65 ± 0.15	23.0 ± 0.66	6.30 ± 0.32				
$z = 28.0 \pm 3$		3.68 ± 0.12	21.9 ± 0.88	5.95 ± 0.31				
$z = 58.5 \pm 3.5$		3.39 ± 0.11	25.5 ± 1.08	7.52 ± 0.40				
$z = 85 \pm 5$		4.05 ± 0.13	20.9 ± 0.88	5.16 ± 0.27				
1 $z = 7.5 \pm 2.5$	25	3.75 ± 0.12	23.6 ± 1.29	6.29 ± 0.40	3.57 ± 0.86	22.5 ± 1.33	14.4 ± 3.7	13.9 ± 1.6
Profile 2	50				3.47 ± 0.12	21.3 ± 0.84	14.8 ± 1.6	14.7 ± 1.6
$z = 7.5 \pm 2.5$		3.94 ± 0.14	22.8 ± 1.06	5.79 ± 0.34				
$z = 30.5 \pm 4.5$		3.64 ± 0.12	22.9 ± 1.00	6.29 ± 0.34				
$z = 60.5 \pm 5.5$		3.44 ± 0.12	20.3 ± 0.57	5.90 ± 0.26				
$z = 97.5 \pm 5.5$		2.85 ± 0.10	18.0 ± 0.67	6.32 ± 0.32				
3 $z = 7.5 \pm 2.5$	75	4.26 ± 0.17	26.4 ± 1.17	6.20 ± 0.37	3.85 ± 0.86	24.8 ± 1.25	13.3 ± 3.3	12.6 ± 1.4
Profile 4	100				4.09 ± 0.14	27.3 ± 1.14	12.6 ± 1.3	11.5 ± 1.2
$z = 7.5 \pm 2.5$		4.65 ± 0.17	29.5 ± 2.31	6.34 ± 0.55				
$z = 30 \pm 4$		4.65 ± 0.15	33.7 ± 1.15	7.25 ± 0.34				
$z = 60 \pm 5$		4.13 ± 0.14						
$z = 87 \pm 5$		2.91 ± 0.10	18.8 ± 0.77	6.46 ± 0.35				
5 $z = 7.5 \pm 2.5$	125	4.71 ± 0.17	31.9 ± 1.38	6.77 ± 0.38	4.11 ± 0.86	29.3 ± 1.39	12.5 ± 2.9	10.7 ± 1.2
6 $z = 7.5 \pm 2.5$	-33	3.31 ± 0.12	20.4 ± 0.87	6.16 ± 0.34	3.32 ± 0.86	19.9 ± 1.08	15.5 ± 4.3	15.7 ± 1.8
7 $z = 7.5 \pm 2.5$	-67	3.16 ± 0.11	22.1 ± 0.97	6.99 ± 0.39	3.23 ± 0.86	21.3 ± 1.13	15.9 ± 4.5	14.7 ± 1.7
8 $z = 7.5 \pm 2.5$	-100	2.65 ± 0.09	18.9 ± 1.26	7.13 ± 0.53	2.94 ± 0.86	18.7 ± 1.31	17.5 ± 5.4	16.7 ± 2.0
Mean					3.6 ± 0.6	23.1 ± 1.1	14.5 ± 3.2	13.8 ± 1.6
Buried rock								
WR-c1		0.51 ± 0.06					10–20	
WR-c2		0.75 ± 0.10					7–20	
Beartooth		0.79 ± 0.06					8.5 ± 1.3	

The concentration from each sample and the mean regolith concentration, measured or determined by regression analysis, are shown. The ^{26}Al:^{10}Be ratio for each sample is shown. Minimum rates of regolith production, calculated from mean regolith concentrations and Eq. (22), are also shown. All errors are 1σ standard deviations. Concentration and ratio errors include propagated ratio and concentration errors measured during AMS and ICP/MS analyses. Regolith production calculations include propagated errors (estimated) from the production rate (10%), flux attenuation length (5%) and regolith density (10%).

measured surface values (Table 1, Fig. 7). Most of the mean concentrations, estimated by the regression, are less than the corresponding measured surface concentrations; the greatest difference between estimated mean and measured surface values is ~15% (Table 1, Fig. 7). Whereas estimated mean concentrations are not greatly different from measured surface values, the regression does produce larger error

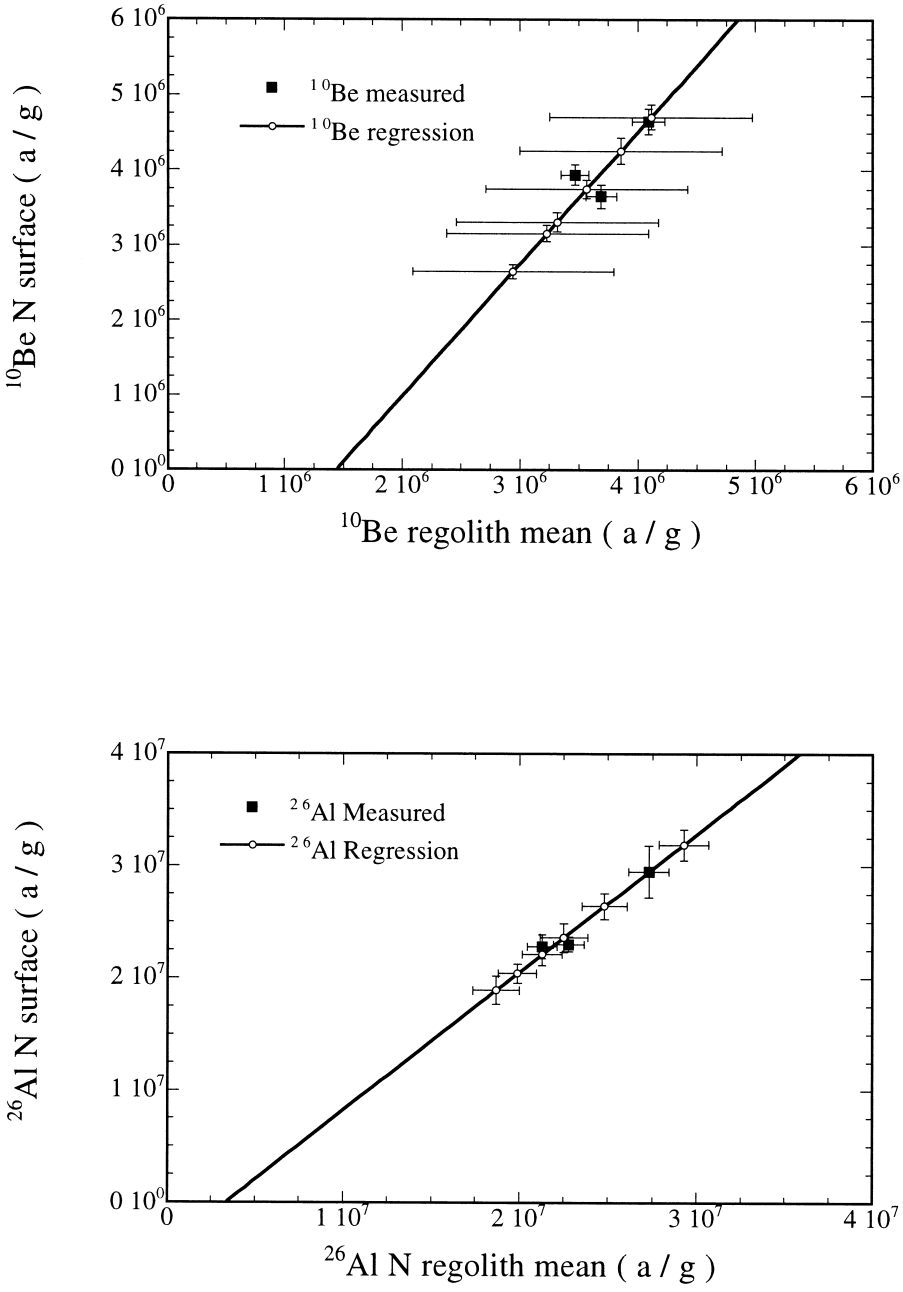

Fig. 7. Top: linear regression from surface ^{10}Be concentration to expected mean regolith ^{10}Be concentration. The regression line is calculated from the measured mean and surface concentration at the three depth profiles (filled squares). Bottom: same for ^{26}Al.

estimates. The increase in error magnitude is greater for the ^{10}Be data because the depth profile samples do not as closely approximate a straight line.

5.3. Downslope profile of mean regolith production

We use the measured (in three depth profiles) and estimated (by regression) mean regolith concentrations to deduce mean rates of regolith production along the hillslope, according to Eq. (22). These values represent the mean rates of regolith production averaged over the entire slope uphill from the sample location. Measured and estimated mean regolith concentrations are nearly uniform along the hillslope (Fig. 8). A slight positive trend in mean values occurs down the northern half of the hillslope ($x > 0$), and a negative trend down the southern half. Measured surface concentrations display a similar pattern. Because rates of regolith production are inversely proportional to mean regolith concentration (Eq. (22)), the rate of production of regolith is also uniform across the hillslope, but trends are in opposite directions of the concentration profiles. Based on a *t*-test, we cannot reject the null hypothesis ($\alpha = 0.05$) that mean concentrations or the mean rate of regolith production are constant down the hillslope, except for mean ^{26}Al concentrations (or regolith production rates deduced from these concentrations) which do increase significantly down the northern half only. Whereas measured and estimated mean regolith concentrations (and associated rates of regolith production) are nearly uniform, measured ^{10}Be and ^{26}Al surface concentrations increase down the northern half of the hillslope. This trend is significant at the 95% confidence level. The decrease in surface concentrations on the south side is not.

Local rates of regolith production, determined from upslope-averaged rates at adjacent sampling sites (Fig. 9), are needed to assess if regolith production is uniform down the hillslope, as suggested by Gilbert (1909). Compared to upslope-averaged values, local rates vary more with distance downslope (Fig. 9). Each local value represents the mean rate of production of regolith for the hillslope segment between the sampling site and the next site upslope. As with the mean rates of regolith production, only the local rates of regolith production determined from ^{26}Al concentrations on the northern side change significantly (95% confidence level). Several of the ^{26}Al concentrations that define this significant trend on the northern hillslope, however, are likely erroneously high, based on the ^{26}Al/^{10}Be ratio (> 6.3) (Table 1, Fig. 9). These high ^{26}Al values, which produce the lowest local rates of regolith production on the hillslope, probably indicate analytical errors associated either with the AMS measurement or the measurement of stable aluminum.

If local rates of regolith production determined from these problematic ^{26}Al concentrations are excluded, we cannot reject the hypothesis that the local rate of regolith production is constant along the hillslope (95% confidence level), for both the north and south sections and for values determined from ^{10}Be and ^{26}Al concentrations. The component of the hypothesis of Gilbert (1909) that asserts production of regolith is constant along convex hillslopes with uniform regolith thickness appears to be valid for the hillslope examined here. The mean local rates of regolith production for the entire hillslope deduced from ^{10}Be and ^{26}Al are 14.3 ± 4.0 and 13.0 ± 4.0 m Ma^{-1}, respectively. Because quartz is likely concentrated in the regolith because of more rapid dissolution of other minerals, the rate of regolith production we have measured should be considered a minimum estimate. The actual rate of regolith production is probably not much higher than this estimate because quartz enrichment in the regolith examined here appears to be relatively minor.

5.4. Rates of regolith production from buried bedrock

Rates of regolith production deduced from ^{10}Be concentrations in buried-bedrock are similar to the rate we deduced from regolith concentrations (Table 1). Assuming that the thickness of regolith is steady, the rate of regolith production from buried-bedrock can be deduced from Eq. (22), using the CRN production rate at the regolith–bedrock interface instead of the surface CRN production rate. Because we were only able to measure maximum and minimum estimates of regolith thickness for the two cliff-edge samples in the Wind River range (described above),

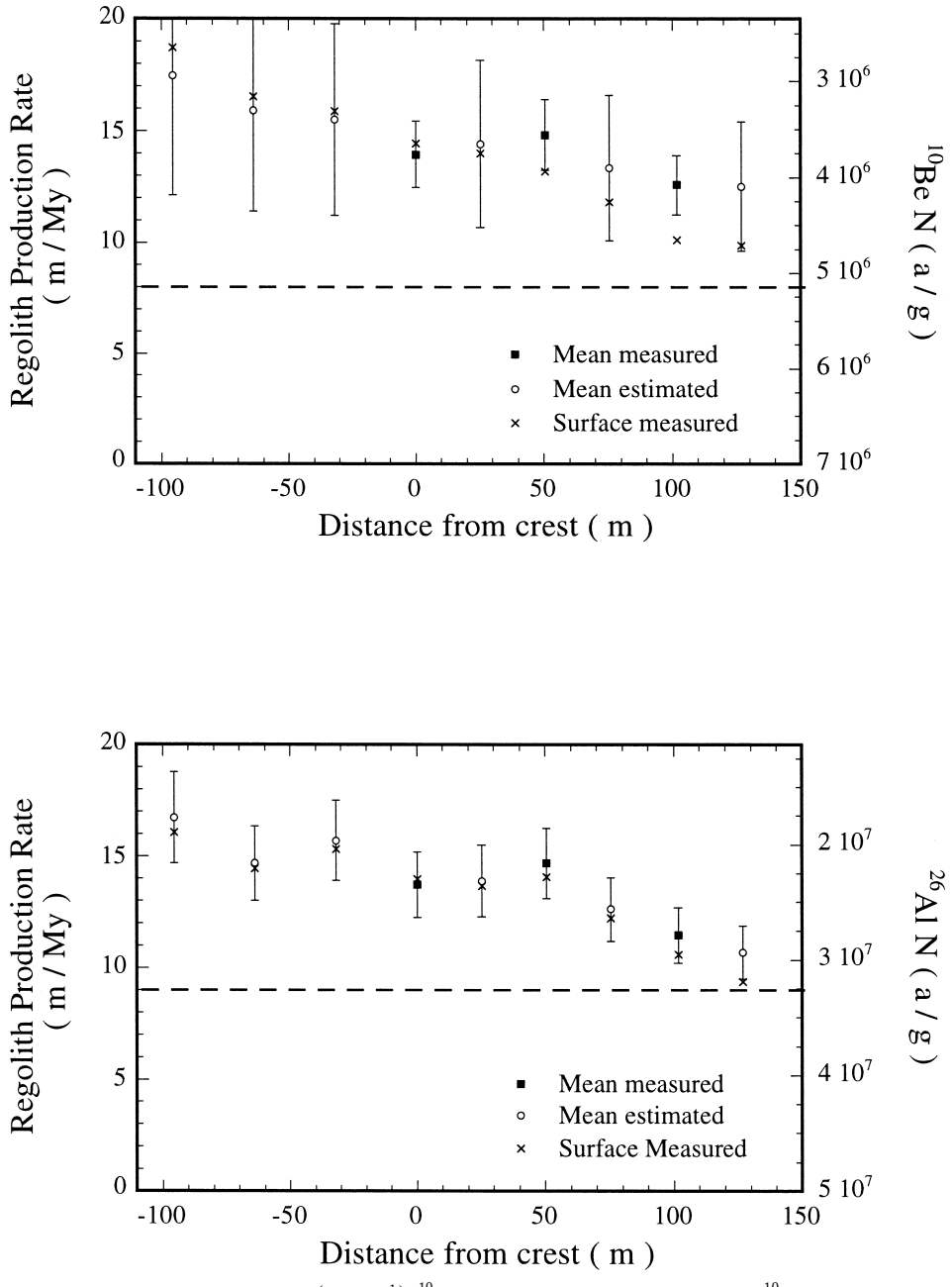

Fig. 8. Top: minimum rates of regolith production (m Ma^{-1}), ^{10}Be mean regolith concentrations, and ^{10}Be surface regolith concentrations along hillslope. Measured mean concentrations from depth profiles and associated rates of regolith production are shown with filled squares. Estimated (by regression) mean concentrations and associated rates of regolith production are shown with open circles. Surface concentrations are shown with xs. The 1σ error bars (see Table 1) for rates of regolith production are included. Error bars for mean and surface concentrations are not included (see Table 1). Dashed line shows the mean rate of bare rock erosion deduced from ^{10}Be concentrations, from 16 samples in the Wind River, Beartooth, and Front Ranges. Bottom: same for ^{26}Al.

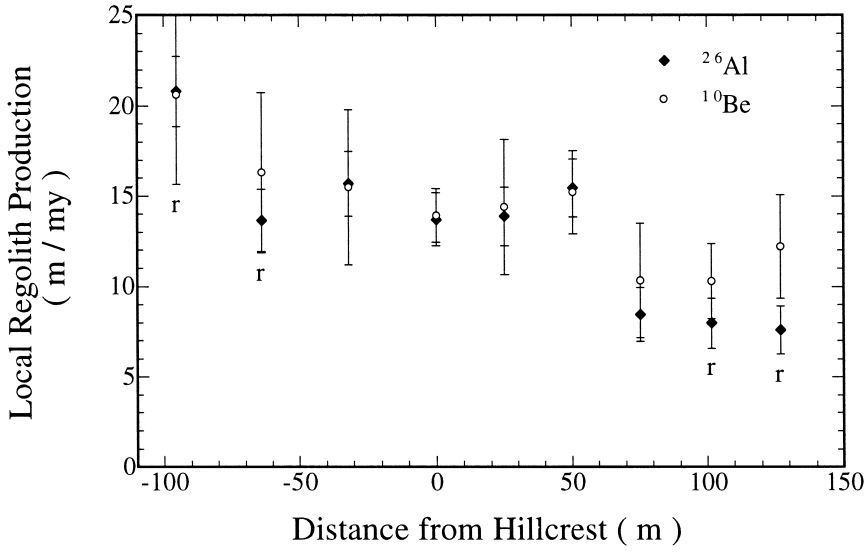

Fig. 9. Local rates of regolith production along hillslope deduced from ^{10}Be and ^{26}Al concentrations. Sample with high (>6.3) ^{26}Al:^{10}Be ratios are indicated by '*r*'.

the estimated rates of regolith production span a broad range, 10–20 and 7–20 m Ma^{-1} (Table 1). The single simple analyzed from a similar hillslope in the Beartooth Range yielded a rate of production of regolith of 8.5 ± 1.3 m Ma^{-1}.

5.5. Hillslope transport and landscape diffusivity

If soil thickness is steady and uniform, hillslope transport must remove all regolith that is produced. Thus, the downslope volume flux at any distance from the hillcrest must equal the volume of regolith produced upslope from that point:

$$Q(x) = (1/\rho_R)\left(\hat{R}(x)\, h(x)\, x\right). \quad (24)$$

Applying our measurements of the rate of production of regolith, the regolith volume flux on the hillslope examined here increases nearly linearly from 0 cm^3 cm^{-1} year^{-1} at the hillcrest to $\sim$22 cm^3 cm^{-1} year^{-1} at distances of $\sim$100–125 m down the hillslope. That the increase is nearly linear is required by the observation that the upslope-average rate of regolith production, $\hat{R}(x)$, is approximately uniform with distance (Fig. 8). The implied long term downslope velocities, ($\hat{u} = Q/h$), averaged over the entire regolith thickness ($h = 90$ cm), vary from 0.0 to $\sim$2.5 mm year^{-1}.

Previous direct measurements of hillslope transport in alpine or periglacial settings have been limited to observations of surface displacement over periods of several years. Typical surface velocities on comparable slopes of several degrees are $\sim$20 mm year^{-1} (Jahn, 1960). Previous estimates of regolith volume flux, Q, which are usually based on surface velocity measurements and in most cases simple assumptions about the shape of the velocity profile with depth, vary from 5–50 cm^3 cm^{-1} year^{-1} (reviewed by Young (1960)). Those from non-periglacial environments are an order of magnitude lower, ranging from 0.5–5 cm^3 cm^{-1} year^{-1} (Young, 1960). Our estimates of long term regolith volume flux, based on the assumption of steady regolith thickness, fall within the range of previous estimates from periglacial environments.

Because the hillslope examined here is convex with constant curvature and regolith production and thickness are uniform, the regolith volume flux must be proportional to the local slope of the hillside (Eq. (22)) (Fig. 10). This is consistent with the argument of Gilbert (1909) for the origin of convex hilltops. The calculated landscape diffusion coefficients, κ, are 182 ± 20 and 169 ± 14 cm^2 year^{-1}, for ^{10}Be and ^{26}Al, respectively. For comparison, in Santa Cruz County, CA, paleo-sea cliffs evolve with a

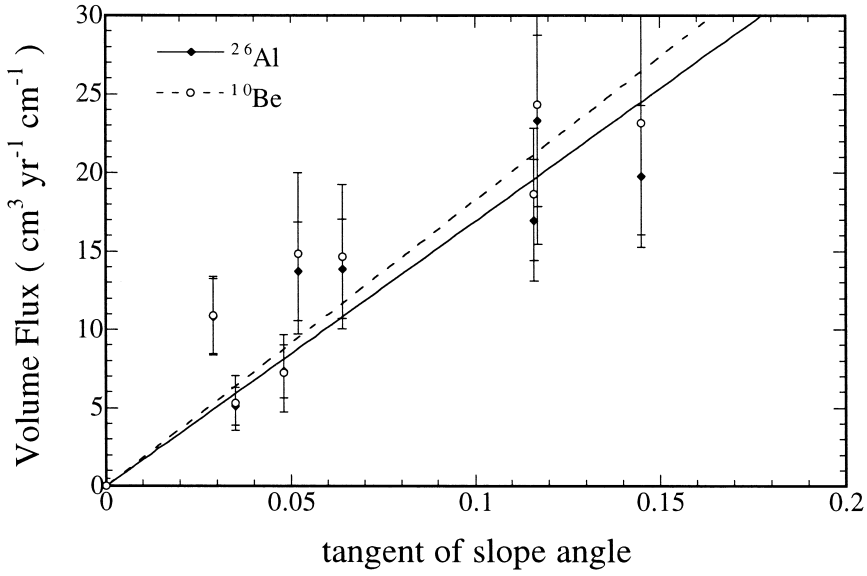

Fig. 10. Volume flux of regolith vs. tangent of slope angle for north and south segments of the hillslope. Regression lines are fit through the origin and are weighted by errors on each measurement. Separate regression lines are calculated for ^{10}Be and ^{26}Al.

topographic diffusivity of 100–110 cm^2 year^{-1} (Rosenbloom and Anderson, 1994), whereas coarser textured hillslopes in coastal California evolve with a diffusivity of 42 ± 23 cm^2 year^{-1} (Reneau, 1988). The diffusivity of clay-rich soils in coastal California is 360 ± 55 cm^2 year^{-1} (McKean et al., 1993).

5.6. Comparison with bare rock erosion rates

Small et al. (1997) documented rates of bare rock erosion using CRN concentrations in the Wind River, Beartooth, and Front Range. All samples were taken from tors and boulders located on summit flats similar to the one on which the hillslope examined here resides. An estimate of the rate of erosion for a single tor or boulder may differ substantially from the actual long-term rate of erosion because these features erode by the episodic removal of blocks or chips. The mean value of many steady-state erosion rate measurements, however, provides a good estimate of the true long-term erosion rate of bare rock, even when the model of steady-state erosion is applied to episodically eroding outcrops (Small et al., 1997). The mean rates of bare rock erosion derived from the seven Wind River range samples are 6.9 ± 2.8 and 8.1 ± 3.3 m Ma^{-1}, for ^{10}Be and ^{26}Al, respectively. Several of the Wind River Range samples were taken from within 1 km of the study site. Rates of bare rock erosion from the other western North American ranges are similar (Fig. 11). On bare rock

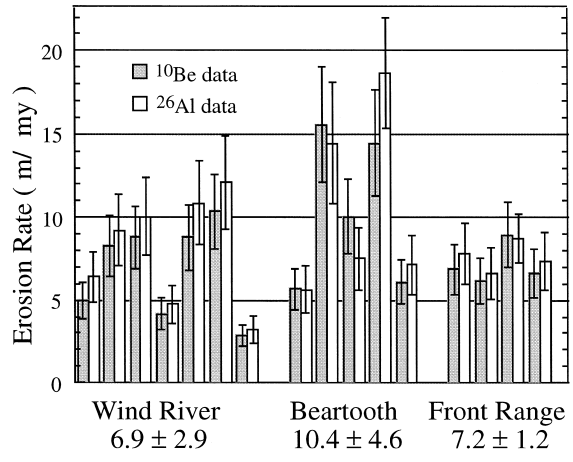

Fig. 11. ^{10}Be and ^{26}Al maximum rates of erosion from summit flat tors and boulders. The rock type, elevation, and sample type (tor or boulder) of each measurement are shown in the work of Small et al. (1997). Error bars for each sample are 1σ standard deviations, and include propagated errors from the production rate, flux attenuation length, rock density, and ratio and concentration measurements. The maximum mean rate of erosion for all samples is 7.6 ± 3.9 m Ma^{-1}.

outcrops, the rate of erosion or surface lowering is equivalent to the rate of regolith production (by definition). We can, therefore, compare these rates with the rates of regolith production we have presented herein. Because the rates of bare rock erosion and regolith production were not measured in the exact same location (>1 km apart), site-to-site variability could introduce some differences. In the alpine environment examined here, the rate of regolith production beneath ~ 90 cm of regolith is nearly twice as fast as the average rate of regolith production on bare rock surfaces (Small et al., 1997). This quantitatively supports the long-standing hypothesis, based on qualitative observations in diverse environments, that bare, exposed bedrock weathers more slowly than rock that is buried by a mantle of regolith (Gilbert, 1877; Wahrhaftig, 1965; Twidale, 1983).

Gilbert (1877) suggested that bare rock weathers more slowly than regolith-mantled rock because liquid water, essential for many weathering processes, is quickly removed from exposed rock surfaces, but can be retained in long term contact with the bedrock interface beneath a regolith mantle. We have observed this distribution of water on summit flats, and it is likely this way for two reasons. First, bare rock on summit flats is located at points of topographic divergence where the influx of water is limited to direct atmospheric input, whereas regolith-mantled rock has access to more water because of its location along flow paths of surface and subsurface water. Second, water evaporates quickly off bare rock, whereas evaporation from regolith is reduced by the moisture conveyance properties of the soil. Frost action, in conjunction with chemical dissolution along fractures and mineral grain boundaries, is likely the primary weathering process that converts bedrock to regolith on summit flats. Regardless of the details of the processes of frost weathering, ample water is required for freezing temperatures to break apart rock (McGreevy and Whalley, 1985; Walder and Hallet, 1985). We hypothesize that regolith-mantled rock weathers more rapidly than bare rock in the alpine environment examined here because the water required for frost weathering is limited on bare rock surfaces.

The discrepancy between the rates of bare and regolith-mantled rock weathering has implications for the time scale of summit flat evolution. Typically, the tallest tors on summit flats protrude about 10–15 m above the surrounding regolith-mantled surface. The rate at which tor height increases is set by the difference between the lowering rates of bare and regolith-mantled rock, which is approximately 5 m Ma^{-1}. If the rate of tor growth has remained constant, the present height of the largest tors indicates that the growth of tors has persisted at most for 2–3 Ma, which is a rough estimate of the time scale on which summit flats have evolved. This supports the hypothesis that the onset or enhancement of alpine glaciation in western US mountain ranges, several million years ago, forced valleys to deepen and isolate summit flats (Small and Anderson, 1998).

6. Conclusions

(1) Based on the assumption that the thickness of regolith is steady, the mean rates of regolith production for a hillslope in the Wind River Range are 14.3 ± 4.0 and 13.0 ± 4.0 m Ma^{-1}, deduced from ^{10}Be and ^{26}Al, respectively. This is supported by rates of regolith production determined from ^{10}Be concentrations in regolith-mantled bedrock.

(2) Rates of regolith production are about twice as fast as rates of bare rock erosion in the alpine environment examined here, most likely because the near-absence of liquid water on bare rock surfaces inhibits frost weathering.

(3) We cannot reject the hypothesis of Gilbert (1909) of a dynamic steady state—the hillslope is convex with uniform curvature and regolith production and thickness are uniform along the slope. If the height of tors and the difference between the weathering rates of bare and regolith-mantled rock provide a fair estimate of the age of summit flats, steady-state hillslope conditions have been attained in less than several million years.

Acknowledgements

This research was supported by a grant from the Topography and Surface Change Program of NASA, and by a graduate fellowship to E. Small from the National Department of Defense. We thank J. Repka, G. Pratt, M. Munkée and Q. Lindh for assistance. We also thank Darryl Granger and an anonymous reviewer for helpful comments.

References

Bierman, P.R., 1994. Using in situ cosmogenic isotopes to estimate rates of landscape evolution: a review from the geomorphic perspective. Journal of Geophysical Research 99 (B7), 13885–13896.

Bierman, P., Steig, E.J., 1996. Estimating rates of denudation using cosmogenic isotope abundances in sediment. Earth Surface Processes and Landforms 21, 125–139.

Brown, E.T., Brook, E.J., Raisbeck, G.M., Yiou, F., Kurz, M.D., 1992. Effective attenuation lengths of cosmic rays producing ^{10}Be and ^{26}Al in quartz: implications for exposure age dating. Geophysical Research Letters 19, 369–372.

Brown, E.T., Stallard, R.F., Larsen, M.C., Raisbeck, G.M., Yiou, F., 1995. Denudation rates determined from the accumulation of in situ-produced ^{10}Be in the Luquillo Experimental Forest, Puerto Rico. Earth and Planetary Science Letters 129, 193–202.

Clark, D.H., Bierman, P.R., Larsen, P., 1995. Improving in situ cosmogenic chronometers. Quaternary Research (New York) 44 (3), 367–377.

Davis, J.C., Proctor, I.D., Southon, J.R., Caffee, M.W., Heikkinen, D.W., Roberts, M.L., Moore, K.W., Turteltaub, K.W., Nelson, D.E., Loyd, D.H., Vogel, J.S., 1990. LLNL/UC AMS facility and research program. Nuclear Instruments and Methods in Physics Research B 52, 269–272.

Elmore, D., Phillips, F., 1987. Accelerator mass spectrometry for measurement of long-lived radioisotopes. Science 236, 543–550.

Gilbert, G.K., 1877. Geology of the Henry Mountains (Utah): US Geographical and Geological Survey of the Rocky Mountains Region, 160 pp.

Gilbert, G.K., 1909. The convexity of hilltops. Journal of Geology 17, 344–350.

Granger, D.E., Kirchner, J.W., Finkel, R., 1996. Spatially averaged long-term erosion rates measured from in situ-produced cosmogenic nuclides in alluvial sediment. Journal of Geology 104, 249–257.

Hallet, B., Putkonen, J., 1994. Surface dating of dynamic landforms. Science 265, 937–940.

Heimsath, A.M., Dietrich, W.E., Nishiizumi, K., Finkel, R.C., 1997. The soil production function and landscape equilibrium. Nature 388, 358–361.

Jahn, A., 1960. Some remarks on evolution of slopes on Spitsbergen. Z. Geomorph. Suppl. 1, 49–58.

Kohl, C.P., Nishiizumi, K., 1992. Chemical isolation of quartz for measurement of in situ-produced cosmogenic nuclides. Geochimica et Cosmochimica Acta 56, 3583–3587.

Lal, D., 1991. Cosmic ray labeling of erosion surfaces: in situ production rates and erosion models. Earth and Planetary Science Letters 104, 424–439.

Lal, D., Peters, B., 1967. Cosmic-ray produced radioactivity on the earth. In: Flugge, S. (Ed.), Handbook of Physics. Springer-Verlag, Berlin, pp. 551–612.

Lasaga, A.C., Solder, J.M., Ganor, J., Burch, T.E., 1994. Chemical weathering rate laws and global geochemical cycles. Geochimica et Cosmochimica Acta 58, 2361–2386.

McGreevy, J.P., Whalley, W.B., 1985. Rock moisture content and frost weathering under natural and experimental conditions: a comparative discussion. Arctic and Alpine Research 17, 337–346.

McKean, J.A., Dietrich, W.E., Finkel, R.C., Southon, J.R., Caffee, M.W., 1993. Quantification of soil production and downslope creep rates from cosmogenic ^{10}Be accumulations on a hillslope profile. Geology 21, 343–346.

Monaghan, M.C., McKean, J., Dietrich, W., Klein, J., 1992. ^{10}Be chronometry of bedrock-to-soil conversion rates. Earth and Planetary Science Letters 111, 483–492.

Nishiizumi, K., 1994. Cosmogenic production of ^{10}Be and ^{26}Al on the surface of the Earth and underground. Abstracts of the Eight International Conference on Geochronology, Cosmochronology, and Isotope Geology. US Geological Survey Circular 1107, 234.

Nishiizumi, K., Winterer, E.L., Kohl, C.P., Klein, J., Middleton, R., Lal, D., Arnold, J.R., 1989. Cosmic ray production rates of ^{10}Be and ^{26}Al in quartz from glacially polished rocks. Journal of Geophysical Research 94 (B12), 17907–17915.

Nishiizumi, K., Finkel, R.C., Klein, J., Kohl, C.P., 1996. Cosmogenic production of Be-7 and Be-10 in water targets. Journal of Geophysical Research 101, 22225–22232.

Porter, S.C., Pierce, K.L., Hamilton, T.D., 1982. Late Wisconsin mountain glaciation in the western United States. In: Porter, S.C. (Ed.), Late Quaternary Environments of the United States, The Late Pleistocene, Vol. 2, pp. 71–111.

Reneau, S.L., 1988. Depositional and erosional history of hollows: applications to landslide location and frequency, long-term erosion rates, and the effects of climatic change. PhD Thesis. University of California, 328 pp.

Rosenbloom, N.S., Anderson, R.C., 1994. Hillslope and channel evolution in a marine terraced landscape, Santa Cruz, California. Journal of Geophysical Research 99, 14013–14029.

Small, E.E., Anderson, R.S., Repka, J.L., Finkel, R., 1997. Erosion rates of alpine bedrock summit surfaces deduced from in situ ^{10}Be and ^{26}Al. Earth and Planetary Science Letters 150, 413–425.

Small, E.E., Anderson, R.S., 1998. Pleistocene relief production in Laramide mountain ranges, western United States. Geology 26, 123–126.

Twidale, C.R., 1983. The research frontier and beyond: granitic terrains. Geomorphology 7, 187–223.

Walder, J., Hallet, B., 1985. A theoretical model of the fracture of rock during freezing. Geological Society of America Bulletin 96, 336–346.

Wahrhaftig, C., 1965. Stepped topography of the southern Sierra Nevada, California. Geological Society of America Bulletin 76, 1165–1190.

York, D., 1966. Least-squares fitting of a straight line. Canadian Journal of Physics 44, 1079–1090.

Young, A., 1960. Soil movement by denudational processes on slopes. Nature 188, 120–122.